JOURNAL OF SOLID STATE CHEMISTRY **130,** 110–116 (1997)
ARTICLE NO. SC977286

Structure and Raman Spectra of Layered Titanium Oxides

Song-Ho Byeon,[1] Sung-Ohk Lee, and Hongdoo Kim

Department of Chemistry, College of Natural Sciences, Kyung Hee University, Kyung Ki 449-701, Korea

Received August 19, 1996; in revised form January 14, 1997; accepted January 22, 1997

The Raman spectra of layered titanium oxides, $NaLnTiO_4$, $Na_2Ln_2Ti_3O_{10}$, $HLnTiO_4$, and $HLnTiO_4 \cdot xH_2O$ (Ln = lanthanides), were investigated. The assignment of the Raman bands was based on the structural data. The characteristic major band around 900 cm^{-1} of parent sodium compounds, which is assigned to the symmetric stretching mode of a short Ti–O bond, was not observed for proton-exchanged derivatives but instead a broad weak band around 820 cm^{-1} appeared. Such a change is proposed to result from the replacement of an ionic Ti–O^-Na^+ bond by a covalent Ti–O–H bond. The difference in Brønsted acidity between titanium oxides and niobium oxides with similar structure could be explained by comparison of their Raman spectra before and after proton exchanges. A structural rearrangement by the intercalation of a water molecule into a proton layer gave two bands around 770 and 900 cm^{-1}, which were assigned to two types of terminal Ti–O bonds with different bond orders. In addition, several characteristic modes of layered-type titanium oxides were systematically compared and assigned. © 1997 Academic Press

INTRODUCTION

Layered oxides with structures related to that of perovskite can be generally formulated $A_m[A'_{n-1}B_nO_{3n+1}]$, where $A'_{n-1}B_nO_{3n+1}$ is the perovskite-type layer and A is an interlayer cation. Each layer has corner-shared BO_6 octahedra with different extents of distortion. The large A' cations occupy 12-coordinate sites as found in the perovskite lattice. The thickness of each perovskite layer is then given by the value of n that determines the number of BO_6 octahedra corner-shared perpendicular to the layers. When the layer charge is low ($m = 1$), the A cations occupy tetragonal prismatic, trigonal prismatic, or tetrahedral sites depending on their size. While a large Tl, Rb, or Cs occupies the tetragonal prismatic site, for instance, a smaller K occupies the trigonal prismatic site of $ACa_2Nb_3O_{10}$ (A = K, Rb, Cs, Tl) with low layer charge density (1, 2). Many compounds of this structure were observed to exchange interlayer cations in molten salt or under acidic conditions (3–5). If the layer charge density is higher, the A cations then occupy 9-coordinate sites between the perovskite layers (6). Most of the phases of this general type contain two interlayer A cations ($m = 2$) per formular unit and have shown no interlayer reaction chemistry. Only a few examples are found to be reactive for ion exchange in the literature; $A_2Ln_2Ti_3O_{10}$ (A = K or Rb, Ln = lanthanides) exhibiting easy ion exchange of the alkali metal in aqueous or molten salt media were reported (7). Another compound similar to those with $m = 2$, $NaLnTiO_4$ (Ln = lanthanides) (8), was also observed to exchange the interlayer sodium ion with lithium (9), silver (10), and proton (11). The difference in reactivity for ion exchange between the compounds with $m = 1$ and $m = 2$ had been understood to be similar to that between the readily exchangeable smectite of low interlayer cation density and the hardly exchangeable micas of higher interlayer cation density (12).

The compounds with $m = 1$ and $m = 2$ also show very different intercalation reactivity of organic bases into the layers. For instance, $HCa_2Nb_3O_{10}$ ($m = 1$) reacts with the weak bases such as pyridine and aniline (13), while $H_2La_2Ti_3O_{10}$ ($m = 2$) does not intercalate even stronger bases such as alkylamines (14). However, such a difference was proposed to be independent of the interlayer cation density but dependent on the nature of the octahedra to which the protons are connected; the protons attached to TiO_6 octahedra are assumed to be less acidic than those attached to NbO_6 octahedra. The acidity of $HCa_2Nb_3O_{10}$, therefore, could be controlled by incorporation of Ti in the Nb site. A general trend showing that protonated niobium oxides are more acidic than protonated niobium–titanium oxides, which have higher acidity than protonated titanium analogs (13, 15), supported this assumption.

In this study, various layered titanium oxides and their protonated and hydrated derivatives with different thicknesses of perovskite layer, $NaLnTiO_4$, $Na_2Ln_2Ti_3O_{10}$, $HLnTiO_4$, and $HLnTiO_4 \cdot xH_2O$ (Ln = La, Nd, Sm, Gd), were systematically characterized by Raman spectroscopy. To investigate the main factor deciding the relative acidity, all the Raman spectra were compared with those of niobium compounds with similar structure. Interestingly,

[1] To whom correspondence should be addressed.

0022-4596/97 $25.00

the Raman spectra of $NaLnTiO_4$ and $Na_2Ln_2Ti_3O_{10}$ resemble in several aspects those of $KCa_2Nb_3O_{10}$, $HCa_2Nb_3O_{10}$, and $HCa_2Nb_3O_{10} \cdot xH_2O$ (16). As previously reported, the sodium ion of $NaLnTiO_4$ and $Na_2Ln_2Ti_3O_{10}$ is exchanged by a proton in a topochemical reaction (7, 11), while proton exchange of $KCa_2Nb_3O_{10}$ is accompanied by structural rearrangement (3). If there is a large difference in Brønsted acidity between layered titanium oxides and niobium oxides, therefore, it can be expected that the Raman spectra of their protonated derivatives will be considerably different from each other. From this comparison, we could successfully assign several characteristic modes of layered-type titanium oxides and explain the difference in Brønsted acidity between titanium oxides and niobium oxides with similar structure. Such results could be used to assign the vibrational modes of other titanium oxides with potential applications as acid catalysts and photocatalysts.

EXPERIMENTAL

$NaLnTiO_4$ (Ln = La, Nd, Sm, and Gd) and $Na_2Ln_2Ti_3O_{10}$ (Ln = La, Nd, Sm, and Gd) were prepared as previously described (7, 8). The stoichiometric amounts of Ln_2O_3, TiO_2, and 20% excess of Na_2CO_3 were mixed, slowly heated to 800°C (2°C/min), and kept constant for 12 h in air. The residual powder was ground, heated at 900°C (for $NaLnTiO_4$) or at 1050°C (for $Na_2Ln_2Ti_3O_{10}$) with intermittent grinding for 2 days, and cooled in the furnace. After the reaction, the products were washed with distilled water and dried at 120°C.

The parent $NaLnTiO_4$ oxides were converted to the hydrogen analogs by ion exchange in aqueous acid (11). $NaLnTiO4$ was stirred in 0.05–0.1 N HNO_3 solution for 24 h at room temperature. The product was filtered, washed with distilled water, and dried at 120°C for 1 h. Hydrated forms of $HLaTiO_4$ and $HSmTiO_4$ were obtained when the sample was dried at room temperature after exchange rather than at 120°C. From several thermogravimetric analyses, the average compositions of hydrated forms were close to $HLaTiO_4 \cdot 0.4H_2O$ and $HSmTiO_4 \cdot 0.5H_2O$, respectively.

A double monochromator (Jobin-Ybon Model U1000) with a photon counter (Stanford Model SR400) was used to obtain Raman spectra. The samples were excited by the 488-nm line of the Ar^+ laser (Lexel Model 95) with 10 mW of power. The laser beam was focused on the sample and the scattered light was collimated into the spectrometer by 180° angle configuration. The Raman spectra were collected at room temperature and analyzed with Igor Pro software (WaveMetrics). The overall spectral resolution of the spectra was determined to be about 2 cm^{-1}.

RESULTS AND DISCUSSION

X-ray diffraction patterns of all the compounds prepared for this work were indexed based on tetragonal symmetry, and estimated unit cell parameters are listed in Table 1. As previously mentioned (11), a c-axis doubling by water intercalation was observed in $HLaTiO_4 \cdot 0.4H_2O$ and $HSmTiO_4 \cdot 0.5H_2O$. The structures of $NaLnTiO_4$ ($P4/nmm$, $Z = 2$) and $Na_2Ln_2Ti_3O_{10}$ ($I4/mmm$, $Z = 2$) are schematically compared in Fig. 1. The lengths of Ti–O bonds in $NaLaTiO_4$ (8) and $Na_2La_2Ti_3O_{10}$ (17) are illustrated as an example in the boxes of Figs. 1a and 1b, respectively. $NaLnTiO_4$ consists of alternate $(NaO)_2$ and $(LnO)_2$ double layers arranged with a sequence of $-(NaO)_2-TiO_2-(LnO)_2-TiO_2-$ along the c axis. The titanium atoms are displaced out of plane toward $(NaO)_2$ double layers, leading to a considerable distortion of TiO_6 octahedra with a very short Ti–O2 bond (~1.72 Å) and a long Ti–O3 bond (~2.66 Å). $(LnO)_2$ layers are corrugated, while $(NaO)_2$ layers are almost flat. In $Na_2Ln_2Ti_3O_{10}$, triple perovskite-like layers consisting of corner-shared TiO_6 octahedra are separated by the $(NaO)_2$ layers only. As demonstrated in the box of Fig. 1b, a displacement of the Ti atom toward the $(NaO)_2$ double layers results in slightly distorted central TiO_6 octahedra and highly distorted TiO_6 octahedra which are similar to those of $NaLaTiO_4$.

The TiO_6 octahedron in $NaLnTiO_4$ is characterized by C_{4v} symmetry. Assuming that the other external modes are well separated in first approximation, the internal mode analysis of this group reveals $5A_1$, B_1, $2B_2$, and $6E$ symmetry Raman active modes. Since the translations and rotations span the representations $A_1 + 2E$, 11 bands could be expected in the Raman spectra for $NaLnTiO_4$. In Fig. 2, the experimental Raman spectra of $NaLnTiO_4$ (Ln = La, Nd,

TABLE 1
Unit Cell Parameters of Some Layered Titanate Oxides

Compounds	a (Å)	c (Å)
$NaLaTiO_4$	3.77343(4)	13.0178(1)
$NaNdTiO_4$	3.75055(4)	12.8242(1)
$NaSmTiO_4$	3.76127(4)	12.6335(2)
$NaGdTiO_4$	3.77085(7)	12.4644(2)
$HLaTiO_4$	3.7200(1)	12.3012(2)
$HLaTiO_4 \cdot 0.4H_2O$	3.7535(1)	28.1403(7)
$HNdTiO_4$	3.6971(1)	12.0928(1)
$HSmTiO_4$	3.6882(1)	11.9863(2)
$HSmTiO_4 \cdot 0.5H_2O$	3.7253(1)	27.3496(9)
$HGdTiO_4$	3.7000(1)	11.7750(3)
$Na_2La_2Ti_3O_{10}$	3.83608(5)	28.5383(4)
$Na_2Nd_2Ti_3O_{10}$	3.8168(1)	28.2816(8)
$Na_2Sm_2Ti_3O_{10}$	3.8031(1)	28.2337(9)
$Na_2Gd_2Ti_3O_{10}$	3.7872(1)	28.2784(9)

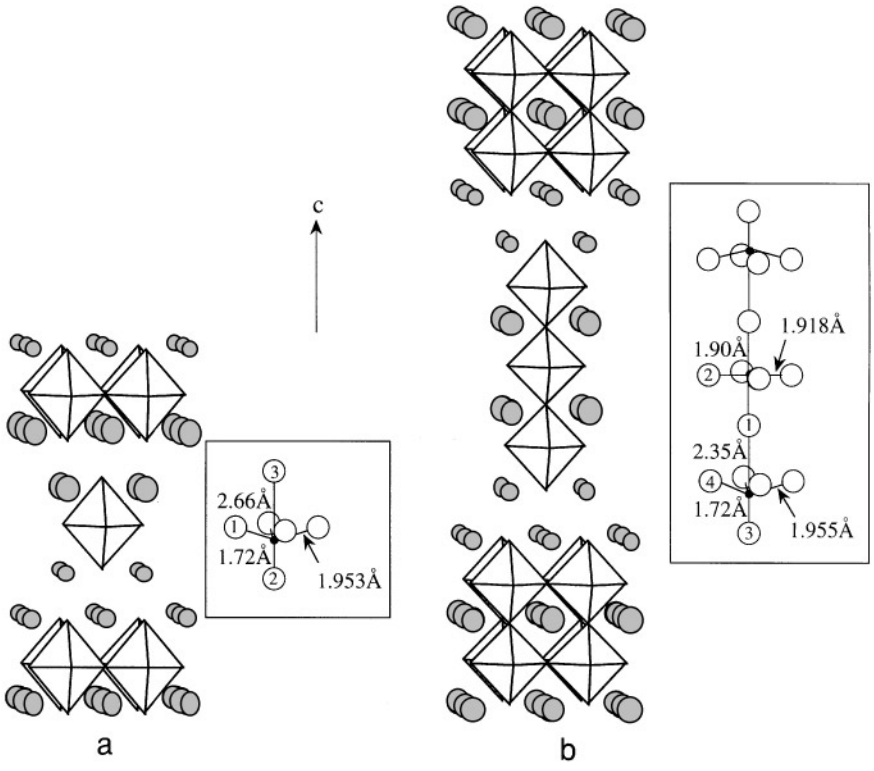

FIG. 1. Schematic illustrations of the structures of (a) $NaLnTiO_4$ and (b) $Na_2Ln_2Ti_3O_{10}$ (*Ln* = lanthanides) perpendicular to the *c* direction of the tetragonal unit cell. The large shaded circles are the *Ln* atoms, and the small shaded circles are the Na atoms. In proton-exchanged analogs, the hydrogen atoms occupy the Na sites. Squares represent TiO_6 octahedra. The Ti–O distances in $NaLaTiO_4$ and $Na_2La_2Ti_2O_{10}$ are introduced in the boxes of (a) and (b), respectively.

Sm, and Gd) are compared as a function of the *Ln* atom. The characteristic Raman bands are visible in the regions 270–340, 520–530, 600–610, and 890–910 cm^{-1}. The Raman bands around 300, 530, and 900 cm^{-1} are not markedly dependent on the *Ln* atoms. The Raman band at 272 cm^{-1} in $NaLaTiO_4$ shifts toward higher wavenumber upon replacement of La by Nd, Sm, and Gd and is superposed to the band around 300 cm^{-1} in $NaSmTiO_4$ (302 cm^{-1}) and $NaGdTiO_4$ (312 cm^{-1}). The frequency of the band around 320–340 cm^{-1} also gradually increases, while the frequency of the band around 600–620 cm^{-1} goes through a maximum for *Ln* = Nd (624 cm^{-1}). From internal mode analysis of the Raman and infrared spectra of $NaLaTiO_4$ and $NaYTiO_4$, Blasse and Van Den Heuvel (18) assigned the strong band around 900 cm^{-1} to the symmetric stretching mode (ν_1) of the short Ti–O bond, the band around 600 cm^{-1} to the asymmetric stretching mode (ν_3), and the bands below 400 cm^{-1} to external modes located in the $(LnO)_2$ layer. Such assignments are in agreement with Fig. 2 and the structural data of $NaLnTiO_4$ (*Ln* = La, Nd, Sm, and Gd) (8). The band around 900 cm^{-1}, which is not observed in the Raman spectra of Sr_2TiO_4, $Sr_3Ti_2O_7$, and $Sr_4Ti_3O_{10}$ with similar arrangement or in other titanium oxides (19), must be related to a very short Ti–O distance (~1.72 Å). This symmetric stretching mode is comparable with that (930 cm^{-1}) of the Nb–O bond with double bond character in $KCa_2Nb_3O_{10}$ (16). The high intensity band around 600 cm^{-1}, which is completely forbidden for the octahedron with inversion symmetry, is also consistent with the strong deviation from the regular TiO_6 octahedron. The differences in position and relative intensity of this band indicate the different extent of octahedral distortion as a function of *Ln* and agree well with the structural data. If we compare Fig. 2 with the bond angles and bond lengths in Table 2, for instance, the most intense band in this region is observed in $NaNdTiO_4$, where O1–Ti–O1 angle (see Fig. 1) is the smallest of those in the four compounds. Moreover, the position of this band changes as a function of the Ti–O1 distance, the highest frequency band being also observed with $NaNdTiO_4$ of the shortest Ti–O1 bond. Such a different extent of distortion would be induced by high flexibility in corrugation of the $(LnO)_2$ layer (8). Although the bands below 400 cm^{-1} could be related to the rock-salt-type layer-related modes (20, 21), the assignments are not straightforward with these spectra. A comparison of the Raman spectra of $NaLnTiO_4$ with those of $Na_2Ln_2Ti_3O_{10}$

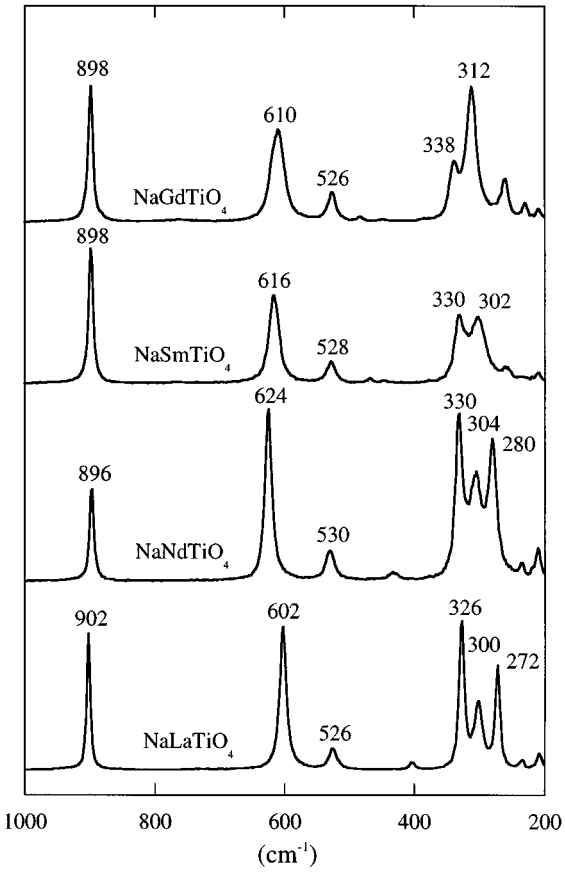

FIG. 2. Raman spectra of NaLnTiO$_4$ (Ln = La, Nd, Sm, and Gd).

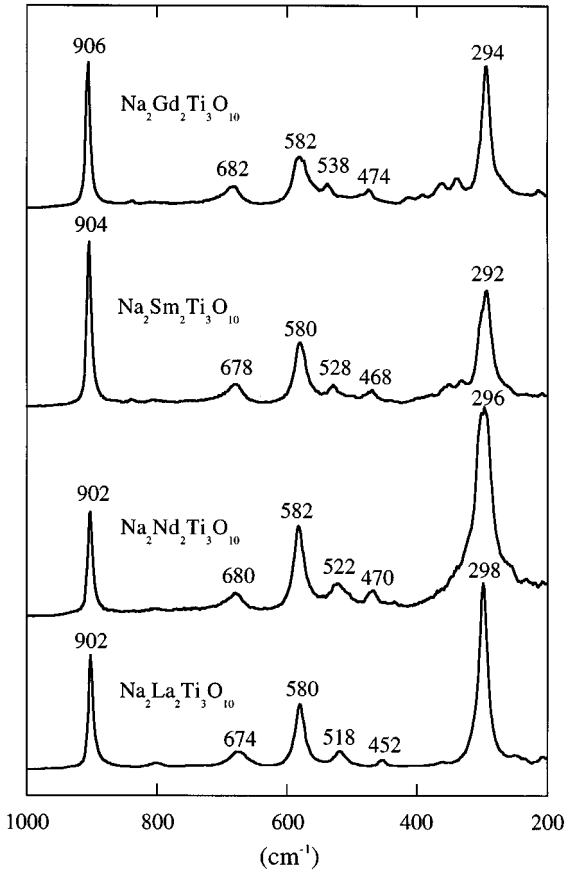

FIG. 3. Raman spectra of $Na_2Ln_2Ti_3O_{10}$ (Ln = La, Nd, Sm, and Gd).

and HLnTiO$_4$ was required to give successful assignments to the bands in this region.

Figure 3 shows the Raman spectra of $Na_2Ln_2Ti_3O_{10}$ (Ln = La, Nd, Sm, and Gd). Similar to the case of NaLnTiO$_4$, a strong sharp band around 900 cm^{-1} is common to all these oxides. The bands around 520 and 580 cm^{-1} are also observed. Unlike NaLnTiO$_4$, however, $Na_2Ln_2Ti_3O_{10}$ possesses only one strong band below 400 cm^{-1} and additional bands in the regions 450–470 and $\sim$680 cm^{-1}. As illustrated in Fig. 1, the structure of $Na_2Ln_2Ti_3O_{10}$ contains a highly distorted TiO_6 octahedron as found in NaLnTiO$_4$ as well as a slightly distorted central one. In addition, there is only a $(NaO)_2$ layer in this structure, all the lanthanide atoms occupying 12-coordinated sites. These structural features reflect the fact that the band around 900 cm^{-1} in Fig. 3 is associated with the symmetric stretching mode of highly distorted TiO_6 octahedra, and the bands around 520 and 580 cm^{-1}, which are also observed around 520 and 600 cm^{-1} in NaLnTiO$_4$, are related to the asymmetric modes of highly distorted TiO_6 octahedra. A change in the intensity of the band around 580 cm^{-1}, similar to that of the band around 600 cm^{-1} of NaLnTiO4, is well correlated with the change of the O4–Ti–O4 bond angle (Table 2). The independence of the band position on the Ln atom agrees with constant Ti–O4 distance within experimental errors. In contrast, the band around 520 cm^{-1} shifts to a higher frequency region from Ln = La to Gd, showing a different tendency from that of the band around 528 cm^{-1} of NaLnTiO$_4$. Such behavior is likely because the central perovskite layer in $Na_2Ln_2Ti_3O_{10}$ is not flexible (8).

TABLE 2
Selected Bond Angles and Bond Lengths of NaLnTiO$_4$ and $Na_2Ln_2Ti_3O_{10}$ (8, 17)

	NaLnTiO$_4$		$Na_2Ln_2Ti_3O_{10}$	
Ln	Bond angle (°) (O1–Ti–O1)	Bond length (Å) (Ti–O1)	Bond angle (°) (O4–Ti–O4)	Bond length (Å) (Ti–O4)
La	154.3	1.953	158.1	1.96
Nd	153.4	1.927	152.1	1.97
Sm	153.8	1.931	152.7	1.96
Gd	153.8	1.936	152.7	1.96

Although the unit cell a parameter does not show any decreasing tendency with $NaLnTiO_4$, that for $Na_2Ln_2Ti_3O_{10}$ gradually decreases when the lanthanide ion becomes smaller, as shown in Table 1. This structural consideration would suggest that the Raman active mode related to the plane perpendicular to the c axis will be dependent on the size of the Ln atom. Additional bands in the regions 450–470 and $\sim 680\ cm^{-1}$, which are absent in the spectra of $NaLnTiO_4$, must consequently be due to the slightly distorted central TiO_6 octahedra. For TiO_6 octahedra with inversion centers, a strong band is generally observed in the 500–720 cm^{-1} region (18, 22, 23). The spectra below 400 cm^{-1} are quite different from those of $NaLnTiO_4$ possessing both $(LnO)_2$ and $(NaO)_2$ layers. When the absence of $(LnO)_2$ layers in $Na_2Ln_2Ti_3O_{10}$ is considered, it is evident that the band around 298 cm^{-1} in Fig. 3 corresponds to the $(NaO)_2$ layer-related mode. The fact that the frequency of this band remains constant despite the change in Ln supports this picture. Hence, it is concluded that the band around 300 cm^{-1} in Fig. 2 is similarly associated with the $(NaO)_2$ layers while the bands that shift from 272 and 326 cm^{-1} to higher wavenumber upon the replacement of La with Nd, Sm, and Gd can be assigned to the $(LnO)_2$ layer-related modes. Such assignments are confirmed again by the scattering patterns of protonated compounds.

The Raman spectra of $HLnTiO_4$ (Ln = La, Nd, Sm, and Gd) are shown in Fig. 4. When these are compared with the spectra of the parent sodium compounds (Fig. 2), two differences in the scattering patterns can be pointed out: (i) Only two bands are visible below 400 cm^{-1}. The band around 300 cm^{-1} that is observed in $NaLnTiO_4$ or $Na_2Ln_2Ti_3O_{10}$ disappears. (ii) The major band around 900 cm^{-1} is absent but a new weak band appears around 820 cm^{-1}. An absence of one band lower than 400 cm^{-1} clearly reflects that an $(NaO)_2$ layer does not exist in $HLnTiO_4$. The gradual shift to higher wavenumber of two bands in this region from Ln = La to Gd is explained by the change in the $(LnO)_2$ layer. The band around 526 cm^{-1} is not influenced by the exchange of a sodium ion with a proton and the position of this band is independent of the Ln atom. The band in the 570–610 cm^{-1} region shows a dependence on Ln similar to that of parent sodium compounds. A decrease in relative intensity and frequency of this band suggests a decrease in TiO_6 octahedral distortion. When the highest frequency band is compared, a marked change is induced by proton exchange. The major Raman band around 900 cm^{-1} for parent $NaLnTiO_4$ disappears and instead a broad band with significantly decreased intensity appears around 820 cm^{-1}, which is almost constant for all the protonated compounds. The disappearance of the band around 900 cm^{-1} must result from the absence of a Ti–O2–Na connection with a very short Ti–O2 bond along the c direction. As a consequence, the appearance of the band around 820 cm^{-1} is associated with the formation of a Ti–O2–H connection in $HLnTiO_4$. Since Raman spectroscopy is sensitive to the bond order in the structure (24, 25), a large shift of the Raman frequency from ~ 900 to $\sim 820\ cm^{-1}$ would suggest a weakening of the Ti–O2 bond. Thus, it can be deduced that an O2–H bond with highly covalent character is formed when sodium forming a highly ionic bond with O2 is replaced by hydrogen. Recently, the Raman spectra of $KCa_2Nb_3O_{10}$ and $HCa_2Nb_3O_{10}$ and its hydrated derivative were investigated (16). A highly distorted NbO_6 octahedron, resembling the TiO_6 octahedron in $NaLnTiO_4$ and $Na_2Ln_2Ti_3O_{10}$, is present in these compounds. While there are terminal Nb–O bonds with double bond character in $KCa_2Nb_3O_{10}$, in contrast, there is no terminal Ti–O bond in $NaLnTiO_4$ and $Na_2Ln_2Ti_3O_{10}$, all the interlayered terminal oxygens form Ti–O–Na bonds. It is surprising

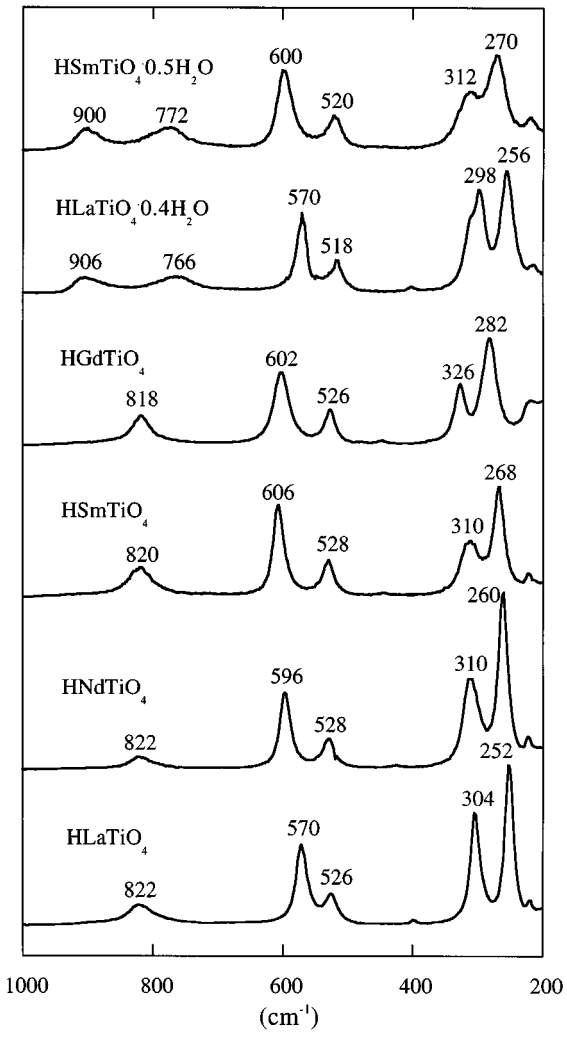

FIG. 4. Raman spectra of $HLnTiO_4$ and $HLnTiO_4 \cdot xH_2O$ (Ln = La, Nd, Sm, and Gd).

that, despite such structural difference, the Raman spectra of these niobium compounds are quite similar to those of layered titanium compounds in this work. Therefore, we expected that the change in the Raman spectra of parent potassium niobium compounds after proton exchange will be similar to that for titanium compounds. Of interest to us, however, is the fact that a strong Raman band at frequency higher than 900 cm^{-1} was observed in a proton-exchanged $HCa_2Nb_3O_{10}$ ($\sim$960 cm^{-1}) as well as a parent $KCa_2Nb_3O_{10}$ ($\sim$930 cm^{-1}). The proton exchange of this compound is accompanied by structural transformation (1, 2). When hydrogen replaces potassium, the interlayered terminal oxygen forms an –OH group that interacts with the terminal oxygen in the adjacent layer by the connection NbO–H $\cdots$ ONb. The observation of a strong band at $\sim$960 cm^{-1} in the Raman spectra of $HCa_2Nb_3O_{10}$ shows that the terminal Nb–O bond order does not decrease after the replacement of terminal Nb–O or Nb–O–K by the Nb–O–H linkage, indicating the low covalent character of the O–H bond. Such a weak O–H bond may explain the higher Brønsted acidity for the niobium compounds than for the titanium compounds with similar structure (14).

The Raman spectra of the hydrated titanium oxides, $HLaTiO_4 \cdot 0.4H_2O$ and $HSmTiO_4 \cdot 0.5H_2O$, are compared with those of homologous compounds in Fig. 4. The vibrational frequencies of the bands at 510–610 cm^{-1} and lower than 400 cm^{-1} remain almost the same as those of unhydrated types. This result suggests that water intercalation does not influence the $(LnO)_2$ layer-related modes and the distortion of TiO_6 octahedra. The band at $\sim$820 cm^{-1} is, however, absent but two broad weak bands are observed at $\sim$770 and $\sim$900 cm^{-1}. This difference is associated with the structural change in the proton layer with hydration. $HLnTiO_4$ retains the structure of parent $NaLnTiO_4$ (Fig. 1), adjacent layers having the staggered conformation shown in Fig. 5a. Due to the relative displacement of the proton layer toward eclipsed conformation, on the contrary, a doubling of the *c* axis is induced with hydration. Such a structural rearrangement is illustrated in Fig. 5b. Considering that the position of the hydrogen atom is variable, two possible explanations could be given. Since the amount of intercalated water ($\sim$0.5 H_2O per formula unit) indicates that about 50% of the possible sites for the water molecule are vacant, it is likely that the band around 900 cm^{-1} is due to the Ti–$O^-H_3O^+$ bond and that around 770 cm^{-1} is due to the Ti–O–H bond. A decrease from $\sim$820 ($HLnTiO_4$) to $\sim$770 cm^{-1} could be induced by an electron density shift from the neighboring Ti–O^- bond. From another point of view, the intercalation of a water molecule into a proton layer is expected to give two types of Ti–O bond along the *c* direction as shown in Fig. 5; one is a terminal Ti–O bond which may have a double bond character, as the Nb–O bond in $KCa_2Nb_3O_{10}$, and the other is also a terminal Ti–O bond but is directly hydrogen bonded to the water molecule. The translation of adjacent layers to form optimum hydrogen bondings is observed in the hydrated types of many protonated oxides (26, 27). Such a hydrogen bonding via a water molecule results in a decrease in the Ti–O bond order and corresponding vibrational frequency. A similar Raman shift with hydration was also observed in $HCa_2Nb_3O_{10} \cdot xH_2O$ (16). Accordingly, the bands at $\sim$770 and $\sim$900 cm^{-1} could be assigned to the Ti–O bond of

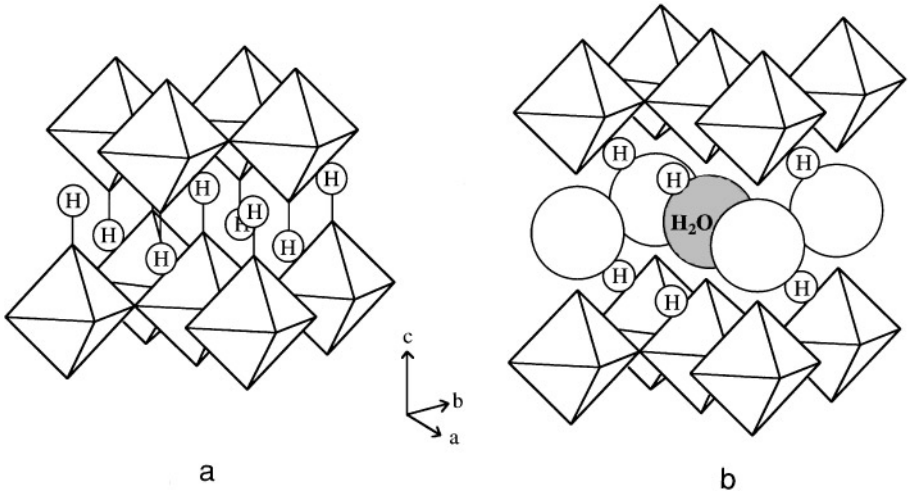

FIG. 5. Idealized representations of proton layers. The octahedra correspond to the TiO_6 unit. (a) $HLnTiO_4$ retains the layered structure of the parent sodium phase, the protons occupying the sodium sites and the adjacent blocks having the staggered conformation. (b) In the hydrated type, $HLnTiO_4 \cdot xH_2O$ (*Ln* = lanthanides, $x \approx 0.5$), the adjacent blocks separated by a proton layer are displaced toward eclipsed conformation of each other. The terminal Ti–O bonds are induced by such displacement; about half of them are directly hydrogen bonded to the water molecule. The large shaded circle is a water molecule intercalated into the layer and the large open circles are vacant sites for water molecules.

lower bond order due to the hydrogen bonding with the water molecule and the terminal Ti–O bond of higher bond order around the vacant site, respectively.

CONCLUSION

When the Raman spectra of $NaLnTiO_4$ and $Na_2Ln_2Ti_3O_{10}$, both of which contain highly distorted TiO_6 octahedra, are compared, the bands around 900 and 580–610 cm^{-1} are assigned to the symmetric stretching and asymmetric stretching modes of distorted TiO_6 octahedra, respectively. If we consider the fact that $NaLnTiO_4$ possesses $(NaO)_2$ and $(LnO)_2$ layers while there are only $(NaO)_2$ layers in $Na_2Ln_2Ti_3O_{10}$, the band at around 300 cm^{-1} observed in both types of compounds can be assigned to the $(NaO)_2$ layer-related mode. The other bands at 200–400 cm^{-1} must consequently be related to the $(LnO)_2$ layer. A large shift of the highest frequency band of $NaLnTiO_4$ toward lower wavenumber, indicating a considerable decrease in Ti–O bond order, is observed upon proton exchange. Weakening of the Ti–O bond along the *c* direction results from the formation of a strong O–H bond. The highly covalent character of the O–H bond makes protonated titanium oxides less acidic than homologous niobium oxides that contain the O–H bond of ionic character. Water intercalation accompanied by structural rearrangement gives two types of Ti–O bonds, which is evidenced by the observation of two bands at around 770 and 900 cm^{-1}. It is expected, therefore, that structural displacement will strongly decrease the covalent character of the O–H bond. The results of this work imply that the intercalation of water into the layer of similar protonated titanium oxides would induce much higher Brønsted acidity.

ACKNOWLEDGMENTS

This work was supported by the Center for Molecular Catalysis, the Korea Science and Engineering Foundation, and the Basic Science Research Institute Program, Ministry of Education (BSRI-96-3421).

REFERENCES

1. M. Dion, M. Ganne, and M. Tournoux, *Mater. Res. Bull.* **16,** 1429 (1981).
2. M. Dion, M. Ganne, M. Tournoux, and J. Ravez, *Rev. Chim. Miner.* **21,** 92 (1984).
3. A. J. Jacobson, J. T. Lewandowski, and J. W. Johnson, *J. Less-Common Met.* **116,** 137 (1986).
4. J. Gopalakrishnan, V. Bhat, and B. Raveau, *Mater. Res. Bull.* **22,** 413 (1987).
5. M. A. Subramanian, J. Gopalakrishnan, and A. W. Sleight, *Mater. Res. Bull.* **23,** 837 (1988).
6. S. N. Ruddlesden and P. Popper, *Acta Crystallogr.* **10,** 538 (1957).
7. J. Gopalakrishnan and V. Bhat, *Inorg. Chem.* **26,** 4299 (1987).
8. S. H. Byeon, K. Park, and M. Itoh, *J. Solid State Chem.* **121,** 430 (1996).
9. K. Toda, S. Kurita, and M. Sato, *J. Ceram. Soc. Jpn.* **104,** 140 (1996).
10. K. Toda, S. Kurita, and M. Sato, *Solid State Ionics* **81,** 267 (1995).
11. S. H. Byeon, J. J. Yoon, and S. O. Lee, *J. Solid State Chem.* **127,** 119 (1996).
12. R. E. Grim, "Clay Mineralogy." McGraw–Hill, New York, 1968.
13. A. J. Jacobson, J. W. Johnson, and J. T. Lewandowski, *Mater. Res. Bull.* **22,** 45 (1987).
14. J. Gopalakrishnan, S. Uma, and V. Bhat, *Chem. Mater.* **5,** 132 (1993).
15. R. Nedjar, M. M. Borel, and B. Raveau, *Z. Anorg. Allg. Chem.* **540–541,** 198 (1986).
16. J. M. Jehng and I. E. Wachs, *Chem. Mater.* **3,** 100 (1991).
17. K. Park and S. H. Byeon, *Bull. Korean Chem. Soc.* **17,** 168 (1996).
18. G. Blasse and G. P. M. Van Den Heuvel, *J. Solid State Chem.* **10,** 206 (1974).
19. G. Burns, F. H. Dacol, G. Kliche, W. Konig, and M. W. Shafer, *Phys. Rev. B* **37,** 3381 (1988).
20. D. Balz and K. Plieth, *Z. Electrochem.* **59,** 545 (1955).
21. A. Rulmont, *Spectrochim. Acta A* **28,** 1287 (1972).
22. J. T. Last, *Phys. Rev.* **105,** 1740 (1957).
23. G. Blasse and A. F. Corsmit, *J. Solid State Chem.* **6,** 513 (1973).
24. A. A. McConnell, J. S. Anderson, and C. N. R. Rao, *Spectrochim. Acta A* **32,** 1067 (1976).
25. F. D. Hardcastle and I. E. Wachs, *Solid State Ionics* **45,** 201 (1991).
26. N. Kumada, O. Horiuchi, F. Muto, and N. Kinomura, *Mater. Res. Bull.* **23,** 209 (1988).
27. N. S. P. Bhuvanesh and J. Gopalakrishnan, *Inorg. Chem.* **34,** 3760 (1995).